

Probing $D_{s0}^*(2317)$ in the decays of B to two charmed mesons

Zhi-Qing Zhang*, Meng-Ge Wang, Yan-Chao Zhao, Zhi-Lin Guan, Na Wang

¹ *Department of Physics, Henan University of Technology,
Zhengzhou, Henan 450052, P. R. China*

(Dated: May 7, 2021)

Abstract

We probe the inner structure of the meson $D_{s0}^*(2317)$ through the decays of $B_{(s)}$ to two charmed mesons within pQCD approach. Assuming $D_{s0}^*(2317)$ as a scalar meson with $\bar{c}s$ structure, we find that the predictions for the branching ratios of the decays $B^+ \rightarrow D_{s0}^{*+}(2317)\bar{D}^{(*)0}$, $B^0 \rightarrow D_{s0}^{*+}(2317)D^{(*)-}$ can explain data within errors. The branching ratios for the decays $B_s \rightarrow D_{s0}^{*+}(2317)D_s^{(*)+}$ are estimated to reach up to 10^{-3} order, which can be observed by the present LHCb and SuperKEKB experiments. In this work, the decay constant of the meson $D_{s0}^*(2317)$ is an input parameter. Unfortunately, its value has been studied by many references but with large uncertainties. Our calculation shows that a smaller decay constant of the meson $D_{s0}^*(2317)$ is supported by compared with the present data, say $55 \sim 70$ MeV. We also calculate the ratios $R_1 = \frac{Br(B^+ \rightarrow D_{s0}^{*+}(2317)\bar{D}^0)}{Br(B^+ \rightarrow D_{s0}^{*+}(2317)\bar{D}^{*0})}$ and $R_2 = \frac{Br(B^0 \rightarrow D_{s0}^{*+}(2317)D^-)}{Br(B^0 \rightarrow D_{s0}^{*+}(2317)D^{*-})}$, which are valuable to determine the inner structure of $D_{s0}^*(2317)$ by compared with the experimental results. Our predictions for the ratios $R_{1,2}$ are consistent with the present data within errors. We expect that these two ratios can be well measured by the future experiments through improving the measurement accuracy for the decays $B^+ \rightarrow D_{s0}^{*+}(2317)\bar{D}^{*0}$ and $B^0 \rightarrow D_{s0}^{*+}(2317)D^{*-}$.

PACS numbers: 13.25.Hw, 12.38.Bx, 14.40.Nd

* e-mail: zhangzhiqing@haut.edu.cn.

I. INTRODUCTION

The charmed-strange meson $D_{s_0}^*(2317)$ was first observed by BABAR Collaboration in the inclusive $D_s^+\pi^0$ invariant mass distribution [1], and confirmed by CLEO [2]. Then BABAR and Belle collaborations probed the properties of this meson through B meson to two charmed-meson decays [3–5]. The branching ratios of these decays measured by BABAR and Belle were averaged by the Particle Data Group (PDG) and given as [6]

$$Br(B^+ \rightarrow D_{s_0}^{*+}(2317)(\rightarrow D_s^+\pi^0)\bar{D}^0) = (8.0_{-1.3}^{+1.6}) \times 10^{-4}, \quad (1)$$

$$Br(B^+ \rightarrow D_{s_0}^{*+}(2317)(\rightarrow D_s^+\pi^0)\bar{D}^{*0}) = (9 \pm 7) \times 10^{-4}, \quad (2)$$

$$Br(B^0 \rightarrow D_{s_0}^{*+}(2317)(\rightarrow D_s^+\pi^0)D^-) = (1.06 \pm 0.16) \times 10^{-3}, \quad (3)$$

$$Br(B^0 \rightarrow D_{s_0}^{*+}(2317)(\rightarrow D_s^+\pi^0)D^{*-}) = (1.5 \pm 0.6) \times 10^{-3}. \quad (4)$$

There have existed some unsettled puzzles since this charmed-strange meson was observed in 2003: First, the low mass puzzle. Its measured mass is at least $150MeV/c^2$ lower than the theoretical calculations from the potential model [7, 8], lattice QCD [9]. Second, the significantly large branching ratio of the decay $D_{s_0}^{*-}(2317) \rightarrow \pi^0 D_s^-$ compared with that of $D_{s_0}^{*-}(2317) \rightarrow \gamma D_s^-$. BESIII measured that $Br(D_{s_0}^{*-}(2317) \rightarrow \pi^0 D_s^-) = 1.00_{-0.14}^{+0.00} \pm 0.14$ [10], which differs from the expectation of the conventional $\bar{c}s$ hypothesis. Third, uncertainties from the decay constant of the meson $D_{s_0}^*(2317)$. It has not been directly determined in experiment, while the theoretical predictions covered a very wide range (shown in Table I). Because of these puzzles, the meson $D_{s_0}^*(2317)$ attracts a lot of at-

TABLE I: The values of $f_{D_{s_0}^*}$ (MeV) given by different references.

	Ref.[11]	Ref.[12]	Ref.[13]	Ref.[14]	Ref.[15]	Ref.[16]	Ref.[17]
$f_{D_{s_0}^*}$	225 ± 25	206 ± 120	200 ± 50	170 ± 20	138 ± 16	$114_{-10.2}^{+11.4}$	118.7
	Ref.[18]	Ref.[19]	Ref.[20]	Ref.[20]	Ref.[21]	Ref.[22]	Ref.[23]
$f_{D_{s_0}^*}$	110 ± 18	$74.4_{-10.6}^{+10.4}$	71	60 ± 13	67 ± 13	67.1 ± 4.5	44

tention. In order to solve these puzzles, many various exotic explanations about its inner structure were proposed, such as DK molecule state [24–28], a tetraquark state [29–32], or a mixture of a $\bar{c}s$ state and a tetraquark state [33–35]. Certainly, its structure was also interpreted as a conventional $\bar{c}s$ scalar meson in many references. For example, some people considered that $D_{s_0}^*(2317)$ is close to the threshold of DK , so the low mass puzzle is because of the coupled-channel effects [36–39]. Sometimes, the spontaneous breaking of chiral symmetry was regarded as another possible reason [40, 41]. Assuming the $D_{s_0}^*(2317)$ as a conventional charmed-strange meson, its properties were studied by using constituent quark model [17], covariant light-front approach [20], QCD sum rules [11, 42], MIT bag model [43], potential model [44–46], Regge trajectories [47] and so on. More detailed discussion can be found in Ref. [48]. Its pionic decay [11] and radiative decay [42] were researched in the light-cone QCD sum rules, and obtained the results being consistent with data. The productions of $D_{s_0}^*(2317)$ in the $B_{(s)}$ decays [17, 49–56] were also discussed. In Ref. [17], the branching ratios of the decays $B \rightarrow D_{s_0}^*(2317)D^{(*)}$ were

calculated in the factorization approximation by using the constituent quark model. The authors found that the meson $D_{s0}^*(2317)$ could be described as a conventional $\bar{c}s$ state by introducing the finite c -quark mass effects.

In order to further reveal the inner structure of $D_{s0}^*(2317)$, we intend to study the weak production of this charmed-strange meson through the two charmed-meson $B_{(s)}$ decays, some of which have been studied by using the light cone sum rules (LCSR) [51] and the relativistic quark model (RQM) [56]. In layout of this paper is as follows. First, in Sec. II, we present the analytic calculations about the $B_{(s)}$ decays to two charmed mesons with $D_{s0}^*(2317)$ involved. Then, we give the numerical results and discussions in Sec. III. A short summary of our results is presented in the final part.

II. THE PERTURBATIVE CALCULATIONS

In the pQCD approach, the only non-perturbative inputs are the light cone distribution amplitudes (LCDAs) and the meson decay constants. For the wave function of the heavy $B_{(s)}$ meson, we take [57, 58]

$$\Phi_{B_{(s)}}(x, b) = \frac{1}{\sqrt{2N_c}}(\not{p}_{B_{(s)}} + m_{B_{(s)}})\gamma_5\phi_{B_{(s)}}(x, b). \quad (5)$$

Here only the contribution of Lorentz structure $\phi_{B_{(s)}}(x, b)$ is taken into account, since the contribution of the second Lorentz structure $\bar{\phi}_{B_{(s)}}$ is numerically small [59] and has been neglected. For the distribution amplitude $\phi_{B_{(s)}}(x, b)$ in Eq.(5), we adopt the following model

$$\phi_{B_{(s)}}(x, b) = N_{B_{(s)}}x^2(1-x)^2 \exp\left[-\frac{M_{B_{(s)}}^2x^2}{2\omega_b^2} - \frac{1}{2}(\omega_b b)^2\right], \quad (6)$$

where ω_b is a free parameter, we take $\omega_b = 0.4 \pm 0.04(0.5 \pm 0.05)$ GeV for $B(B_s)$ in numerical calculations, and $N_B = 101.445(N_{B_s} = 63.671)$ is the normalization factor for $\omega_b = 0.4(0.5)$. For B_s meson, the SU(3) breaking effects are taken into consideration.

The wave functions for the scalar meson D_{s0}^* ¹, we use the form defined in Ref. [55]

$$\langle \bar{D}_{s0}^{*+}(2317)(p_2) | \bar{c}_\beta(z) s_\gamma(0) | 0 \rangle = \frac{1}{\sqrt{2N_c}} \int dx e^{ip_2 \cdot z} [(\not{p}_2)_{lj} + m_{D_{s0}^*} I_{lj}] \phi_{D_{s0}^*}. \quad (7)$$

It is noticed that the distribution amplitudes which associate with the nonlocal operators $\bar{c}(z)\gamma_\mu s$ and $\bar{c}(z)s$ are different. The difference between them is order of $\bar{\Lambda}/m_{D_{s0}^*} \sim (m_{D_{s0}^*} - m_c)/m_{D_{s0}^*}$. If we set $m_{D_{s0}^*} \sim m_c$, we can get these two distribution amplitudes being very similar. For the leading power calculation, it is reasonable to parameterize them in the same form as

$$\phi_{D_{s0}^*}(x) = \tilde{f}_{D_{s0}^*} 6x(1-x) [1 + a(1-2x)] \quad (8)$$

¹ From now on, we will use D_{s0}^* to denote $D_{s0}^*(2317)$ for simply in some places.

in the heavy quark limit. Here the decay constant $\tilde{f}_{D_{s0}^*}$ is defined through the matrix element of the scalar current

$$\langle 0 | \bar{s}c | D_{s0}^*(\mathbf{p}) \rangle = \tilde{f}_{D_{s0}^*} m_{D_{s0}^*} \quad (9)$$

and the shape parameter $a = -0.21$ [51] is fixed under the condition that the distribution amplitude $\phi_{D_{s0}^*}(x)$ possesses the maximum at $x = m_c/m_{D_{s0}^*}$ with $m_c = 1.275$ GeV. It is worthwhile to point out that the intrinsic b dependence of this charmed meson's wave function has been neglected in our analysis.

As for the wave functions of the mesons $D^{(*)}$, we use the form derived in Ref. [60]

$$\int \frac{d^4\omega}{(2\pi)^4} e^{ik\cdot\omega} \langle 0 | \bar{c}_\beta(0) u_\gamma(\omega) | \bar{D}^0 \rangle = -\frac{i}{\sqrt{2N_c}} [(\not{p}_D + m_D)\gamma_5]_{\gamma\beta} \phi_D(x, b), \quad (10)$$

$$\int \frac{d^4\omega}{(2\pi)^4} e^{ik\cdot\omega} \langle 0 | \bar{c}_\beta(0) u_\gamma(\omega) | \bar{D}^{*0} \rangle = -\frac{i}{\sqrt{2N_c}} [(\not{p}_{D^*} + m_{D^*})\not{\epsilon}_L]_{\gamma\beta} \phi_{D^*}^L(x, b), \quad (11)$$

where $\not{\epsilon}_L$ is the longitudinal polarization vector. In this work only the longitudinal polarization component is used. Here we take the best-fitted form $\phi_D^{(*)}$ from B to charmed meson decays derived in [61] as

$$\phi_D(x, b) = \frac{f_D}{2\sqrt{2N_c}} 6x(1-x)[1 + C_D(1-2x)] \exp\left[-\frac{\omega^2 b^2}{2}\right]. \quad (12)$$

For the wave function $\phi_{D_s}(x, b)$, it has the similar expression as $\phi_D(x, b)$ except with the different parameters. These parameters are given as follows: $f_D = 223$ MeV, $f_{D_s} = 274$ MeV, and $C_{D(s)} = 0.5$ (0.4), $\omega_{D(s)} = 0.1$ (0.2) GeV [61]. For the wave function $\phi_{D(s)^*}(x, b)$, we take the same distribution amplitude with that of the pseudoscalar meson $D_{(s)}$ because of their small mass difference. The decay constants f_{D^*} and $f_{D_s^*}$ are given by the relations

$$f_{D^{*-}} = \sqrt{\frac{M_{D^-}}{M_{D^{*-}}}} f_{D^-}, \quad f_{D_s^{*-}} = \sqrt{\frac{M_{D_s^-}}{M_{D_s^{*-}}}} f_{D_s^-}. \quad (13)$$

For these processes considered, the weak effective Hamiltonian H_{eff} can be written as:

$$H_{eff} = \frac{G_F}{\sqrt{2}} \left\{ \sum_{q=u,c} V_{qb} V_{qD}^* [C_1(\mu) O_1^q(\mu) + C_2(\mu) O_2^q(\mu)] - V_{tb} V_{tD}^* \left[\sum_{i=3}^{10} C_i(\mu) O_i(\mu) \right] \right\} + H.C., \quad (14)$$

where $V_{qb(D)}$ and $V_{tb(D)}$ with $D = d, s$ are CKM matrix elements. The local four-quark operators O_i ($i = 1, \dots, 10$) include three type operators: current-current operators ($O_{1,2}^q$),

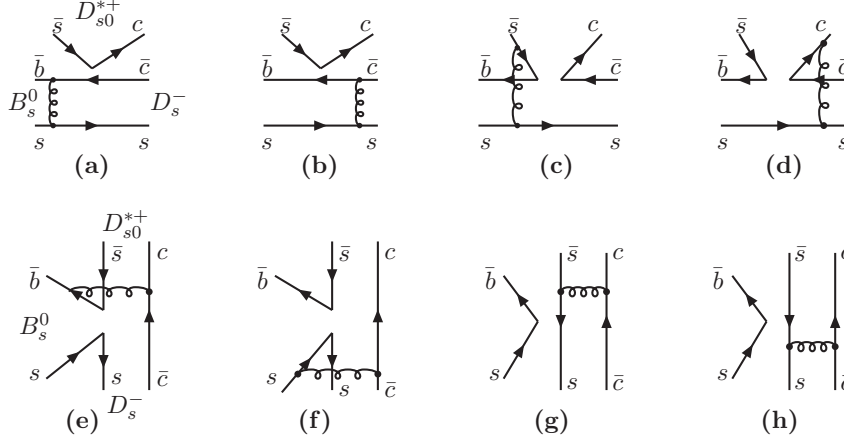


FIG. 1: A part of diagrams contributing to the $B_s^0 \rightarrow D_{s0}^{*+}(2317)D_s^-$ decay.

QCD penguin ($O_{3\sim 6}$) and electroweak penguin operators ($O_{7\sim 10}$),

$$O_1^q = (\bar{q}_\alpha b_\beta)_{V-A} (\bar{D}_\beta q_\alpha)_{V-A}, \quad O_2^q = (\bar{q}_\alpha b_\alpha)_{V-A} (\bar{D}_\beta q_\beta)_{V-A}, \quad (15)$$

$$O_3 = (\bar{D}_\alpha b_\alpha)_{V-A} \sum_{q'} (\bar{q}'_\beta q'_\beta)_{V-A}, \quad O_4 = (\bar{D}_\beta b_\alpha)_{V-A} \sum_{q'} (\bar{q}'_\alpha q'_\beta)_{V-A}, \quad (16)$$

$$O_5 = (\bar{D}_\alpha b_\alpha)_{V-A} \sum_{q'} (\bar{q}'_\beta q'_\beta)_{V+A}, \quad O_6 = (\bar{D}_\beta b_\alpha)_{V-A} \sum_{q'} (\bar{q}'_\alpha q'_\beta)_{V+A}, \quad (17)$$

$$O_7 = \frac{3}{2} (\bar{D}_\alpha b_\alpha)_{V-A} \sum_{q'} e_{q'} (\bar{q}'_\beta q'_\beta)_{V+A}, \quad O_8 = \frac{3}{2} (\bar{D}_\beta b_\alpha)_{V-A} \sum_{q'} e_{q'} (\bar{q}'_\alpha q'_\beta)_{V+A}, \quad (18)$$

$$O_9 = \frac{3}{2} (\bar{D}_\alpha b_\alpha)_{V-A} \sum_{q'} e_{q'} (\bar{q}'_\beta q'_\beta)_{V-A}, \quad O_{10} = \frac{3}{2} (\bar{D}_\beta b_\alpha)_{V-A} \sum_{q'} e_{q'} (\bar{q}'_\alpha q'_\beta)_{V-A}, \quad (19)$$

where $(\bar{q}'_\alpha q'_\beta)_{V\pm A} = \bar{q}'_\alpha \gamma_\nu (1 \pm \gamma_5) q'_\beta$ with α, β being the color indices and q' represent the active quarks at the m_b scale, which can be u, d, s, c and b . We calculate in the light-cone coordinate, where a vector is defined as

$$P_\mu = \left(\frac{P_0 + P_3}{\sqrt{2}}, \frac{P_0 - P_3}{\sqrt{2}}, P_1, P_2 \right). \quad (20)$$

When working in the rest frame of $B_{(s)}$ meson and defining the direction where D_{s0}^* moves as the positive direction of z -axis, we can write the momenta of B, D_{s0}^*, D_s mesons as

$$P_B = \frac{m_B}{\sqrt{2}} (1, 1, \mathbf{0}_\perp), P_{D_{s0}^*} = \frac{m_B}{\sqrt{2}} (1 - r_{D_s}^2, r_{D_{s0}^*}^2, \mathbf{0}_\perp), P_{D_s} = \frac{m_B}{\sqrt{2}} (r_{D_s}^2, 1 - r_{D_{s0}^*}^2, \mathbf{0}_\perp), \quad (21)$$

where $r_{D_{s0}^*} = m_{D_{s0}^*}/m_B, r_{D_s} = m_{D_s}/m_B$ and $\mathbf{0}_\perp$ is zero two-component vector. If using k_1, k_2 , and k_3 to denote the momenta carried by the light quark in B and two charmed mesons, we have

$$k_1 = \left(\frac{m_B}{\sqrt{2}} x_1, 0, \mathbf{k}_{1\perp} \right), k_2 = \left(\frac{m_B}{\sqrt{2}} (1 - r_{D_s}^2) x_2, 0, \mathbf{k}_{2\perp} \right), k_3 = \left(0, \frac{m_B}{\sqrt{2}} (1 - r_{D_{s0}^*}^2) x_3, \mathbf{k}_{3\perp} \right). \quad (22)$$

Here we consider the decays $B_s^0 \rightarrow D_{s_0}^{*+}(2317)D_s^-$ and $B_s^0 \rightarrow D_{s_0}^{*-}(2317)D_s^+$ as examples, which will include all types of Feynman diagram amplitudes we need. For the decay $B_s^0 \rightarrow D_{s_0}^{*+}(2317)D_s^-$, we give a part of its Feynman diagrams at leading order in Fig.1, where the scalar meson is in the emission (upper) position. If changing the positions of $D_{s_0}^{*+}(2317)$ and D_s^- for the annihilation type Feynman diagrams (the second line in Fig.1), we will obtain another part of Feynman diagrams which can also contribute to the decay $B_s^0 \rightarrow D_{s_0}^{*+}(2317)D_s^-$. These Feynman diagrams are given in Fig. 2. The Feynman diagrams for the decay $B_s^0 \rightarrow D_{s_0}^{*-}(2317)D_s^+$ are totally same with those for the decay $B_s^0 \rightarrow D_{s_0}^{*+}(2317)D_s^-$ and can be obtained just by changing $D_{s_0}^{*+}(D_s^-)$ to $D_s^+(D_{s_0}^{*-})$ in Fig.1 and 2. There are two points we need to emphasize: (I) Besides of the different positions for the final states in the annihilation type Feynman diagrams between Fig.1 and 2, another difference is that the former with $c\bar{c}$ pair generated from a hard gluon, while the later with $s\bar{s}$ pair generated. (II) In order to distinguish these amplitudes for the decays $B_s^0 \rightarrow D_{s_0}^{*+}(2317)D_s^-$ and $B_s^0 \rightarrow D_{s_0}^{*-}(2317)D_s^+$ from each other, we add the character "c" in the subscript for each amplitude which corresponds to the Feynman diagram with a conventional charmed meson being the emission (upper) position. For the amplitudes corresponding to the annihilation diagrams with $s\bar{s}$ pair generated from a hard gluon, we add another character "s" in the subscripts. In the following, we give the detail expressions of the Feynman diagram amplitudes for the decay $B_s^0 \rightarrow D_{s_0}^{*+}(2317)D_s^-$. Fig.1(a) and 1(b) are the factorization emission diagrams, Fig.1(c) and 1(d) are the nonfactorization emission ones, the corresponding amplitudes can be written as

$$\begin{aligned} \mathcal{F}_e^{LL} = & 8\pi C_F M_{B_s}^4 f_{D_{s_0}^*} \int_0^1 dx_1 dx_3 \int_0^\infty b_1 db_1 b_3 db_3 \phi_{B_s}(x_1, b_1) \phi_{D_s}(x_3) \\ & \times [1 + r_{D_s} + (1 - 2r_{D_s})x_3] E_e(t_e^{(1)}) S_t(x_3) h_e(x_1, x_3(1 - r_{D_{s_0}^*}^2), b_1, b_3) \\ & + [2(r_c + 1)r_{D_s} - r_c - r_{D_s}^2] E_e(t_e^{(2)}) S_t(x_1) h_e(x_3, x_1(1 - r_{D_{s_0}^*}^2), b_3, b_1)], \end{aligned} \quad (23)$$

$$\begin{aligned} \mathcal{F}_e^{SP} = & 16\pi C_F M_{B_s}^4 f_{D_{s_0}^*} r_{D_{s_0}^*} \int_0^1 dx_1 dx_3 \int_0^\infty b_1 db_1 b_3 db_3 \phi_{B_s}(x_1, b_1) \phi_{D_s}(x_3) \\ & \times [1 + r_{D_s}(2 + r_{D_s} + x_3(1 - 4r_{D_s}))] E_e(t_e^{(1)}) S_t(x_3) h_e(x_1, x_3(1 - r_{D_{s_0}^*}^2), b_1, b_3) \\ & + [-r_c(1 - 4r_{D_s}) + 2r_{D_s}(1 - r_{D_s})] E_e(t_e^{(2)}) S_t(x_1) h_e(x_3, x_1(1 - r_{D_{s_0}^*}^2), b_3, b_1)], \end{aligned} \quad (24)$$

$$\begin{aligned} \mathcal{M}_e^{LL} = & 32\pi C_f m_{B_s}^4 / \sqrt{2N_C} \int_0^1 dx_1 dx_2 dx_3 \int_0^\infty b_1 db_1 b_2 db_2 \phi_{B_s}(x_1, b_1) \phi_{D_s}(x_2) \phi_{D_{s_0}^*}(x_3) \\ & \times \{ [x_2 - r_{D_s}x_3(1 - 2r_{D_s})] E_{en}(t_{en}^{(1)}) h_{en}^{(1)}(x_1, x_2, x_3, b_1, b_2) \\ & + [x_2 - 1 - (1 - r_{D_s})x_3 + r_c r_{D_{s_0}^*}] E_{en}(t_{en}^{(2)}) h_{en}^{(2)}(x_1, x_2, x_3, b_1, b_2) \}, \end{aligned} \quad (25)$$

$$\begin{aligned} \mathcal{M}_e^{LR} = & 32\pi C_f m_{B_s}^4 / \sqrt{2N_C} \int_0^1 dx_1 dx_2 dx_3 \int_0^\infty b_1 db_1 b_2 db_2 \phi_{B_s}(x_1, b_1) \phi_{D_s}(x_2) \phi_{D_{s_0}^*}(x_3) \\ & \times (1 + r_{D_s}) \{ r_{D_{s_0}^*} [x_2 + r_{D_s}(1 + r_{D_s})x_3] E_{en}(t_{en}^{(1)}) h_{en}^{(1)}(x_1, x_2, x_3, b_1, b_2) \\ & - [r_c + r_{D_{s_0}^*}(1 - x_2) + r_{D_s}(r_{D_s} + 1)r_{D_{s_0}^*}x_3] E_{en}(t_{en}^{(2)}) h_{en}^{(2)}(x_1, x_2, x_3, b_1, b_2) \}, \end{aligned} \quad (26)$$

$$\begin{aligned}
\mathcal{M}_e^{SP} &= 32\pi C_f m_{B_s}^4 / \sqrt{2N_C} \int_0^1 dx_1 dx_2 dx_3 \int_0^\infty b_1 db_1 b_2 db_2 \phi_{B_s}(x_1, b_1) \phi_{D_s}(x_2) \phi_{D_{s_0}^*}(x_3) \\
&\times \left\{ [x_2 - (r_{D_{s_0}^*} - 1)x_3] E_{en}(t_{en}^{(1)}) h_{en}^{(1)}(x_1, x_2, x_3, b_1, b_2) \right. \\
&\quad \left. - [1 - x_2 - r_{D_s} x_3 - r_c r_{D_{s_0}^*}] E_{en}(t_{en}^{(2)}) h_{en}^{(2)}(x_1, x_2, x_3, b_1, b_2) \right\}, \tag{27}
\end{aligned}$$

where $r_{D_{s_0}^*} = m_{D_{s_0}^*}/m_{B_s}$, $r_{D_s} = m_{D_s}/m_{B_s}$, $r_c = m_c/m_{B_s}$ and $f_{D_{s_0}^*}$ is the decay constant of the scalar meson $D_{s_0}^*(2317)$. As we know that the double logarithms $\alpha_s \ln^2 x$ produced by the radiative corrections are not small expansion parameters when the end point region is important, in order to improve the perturbative expansion, the threshold resummation of these logarithms to all order is needed, which leads to a quark jet function

$$S_t(x) = \frac{2^{1+2c}\Gamma(3/2+c)}{\sqrt{\pi}\Gamma(1+c)} [x(1-x)]^c, \tag{28}$$

with $c = 0.35$. It is effective to smear the end point singularity with a momentum fraction $x \rightarrow 0$. This factor will also appear in the factorizable annihilation amplitudes.

As to the (non)factorizable annihilation amplitudes for the second line Feynman diagrams in Fig.1 can be obtained by the Feynman rules and are given as

$$\begin{aligned}
\mathcal{M}_{an}^{LL} &= 32\pi C_f m_{B_s}^4 / \sqrt{2N_C} \int_0^1 dx_1 dx_2 dx_3 \int_0^\infty b_1 db_1 b_3 db_3 \phi_{B_s}(x_1, b_1) \phi_{D_{s_0}^*}(x_2) \phi_{D_s}(x_3) \\
&\times \left\{ [x_2 - 1 + r_{D_s} r_{D_{s_0}^*} (x_2 + x_3 - 4)] E_{an}(t_{an}^{(1)}) h_{an}^{(1)}(x_1, x_2, x_3, b_1, b_3) \right. \\
&\quad \left. + [1 - x_3 - r_{D_s} r_{D_{s_0}^*} (x_2 + x_3 - 2)] E_{an}(t_{an}^{(2)}) h_{an}^{(2)}(x_1, x_2, x_3, b_1, b_3) \right\}, \tag{29}
\end{aligned}$$

$$\begin{aligned}
\mathcal{M}_{an}^{LR} &= 32\pi C_f m_{B_s}^4 / \sqrt{2N_C} \int_0^1 dx_1 dx_2 dx_3 \int_0^\infty b_1 db_1 b_3 db_3 \phi_{B_s}(x_1, b_1) \phi_{D_{s_0}^*}(x_2) \phi_{D_s}(x_3) \\
&\times \left\{ [r_{D_{s_0}^*} (x_2 + 1) - r_{D_s} (x_3 + 1)] E_{an}(t_{an}^{(1)}) h_{an}^{(1)}(x_1, x_2, x_3, b_1, b_3) \right. \\
&\quad \left. - [r_{D_s} (1 - x_3) + r_{D_{s_0}^*} (x_2 - 1)] E_{an}(t_{an}^{(2)}) h_{an}^{(2)}(x_1, x_2, x_3, b_1, b_3) \right\}, \tag{30}
\end{aligned}$$

$$\begin{aligned}
\mathcal{M}_{an}^{SP} &= 32\pi C_f m_{B_s}^4 / \sqrt{2N_C} \int_0^1 dx_1 dx_2 dx_3 \int_0^\infty b_1 db_1 b_3 db_3 \phi_{B_s}(x_1, b_1) \phi_{D_{s_0}^*}(x_2) \phi_{D_s}(x_3) \\
&\times \left\{ [1 - x_3 - r_{D_s} r_{D_{s_0}^*} (x_2 + x_3 - 4)] E_{an}(t_{an}^{(1)}) h_{an}^{(1)}(x_1, x_2, x_3, b_1, b_3) \right. \\
&\quad \left. - [1 - x_2 - r_{D_s} r_{D_{s_0}^*} (x_2 + x_3 - 2)] E_{an}(t_{an}^{(2)}) h_{an}^{(2)}(x_1, x_2, x_3, b_1, b_3) \right\}, \tag{31}
\end{aligned}$$

$$\begin{aligned}
\mathcal{F}_a^{LL} &= -\mathcal{F}_a^{LR} = 8\pi C_f f_{B_s} m_{B_s}^4 \int_0^1 dx_2 dx_3 \int_0^\infty b_2 db_2 b_3 db_3 \phi_{D_{s_0}^*}(x_2) \phi_{D_s}(x_3) \\
&\left\{ [x_3 - 1 + 2r_{D_s} r_{D_{s_0}^*} (x_3 - 2)] E_a(t_a^{(1)}) S_t(x_3) h_a(\overline{(1 - r_{D_s}^2)x_2}, \overline{(1 - r_{D_{s_0}^*}^2)x_3}, b_2, b_3) \right. \\
&\quad \left. + [1 - x_2 - 2r_{D_s} r_{D_{s_0}^*} (x_2 - 2)] E_a(t_a^{(2)}) S_t(x_2) h_a(\overline{(1 - r_{D_{s_0}^*}^2)x_3}, \overline{(1 - r_{D_s}^2)x_2}, b_3, b_2) \right\}, \tag{32}
\end{aligned}$$

$$\begin{aligned}
\mathcal{F}_a^{SP} &= 16\pi C_f f_{B_s} m_{B_s}^4 \int_0^1 dx_2 dx_3 \int_0^\infty b_2 db_2 b_3 db_3 \phi_{D_{s_0}^*}(x_2) \phi_{D_s}(x_3) \\
&\left\{ [2r_{D_{s_0}^*} + r_{D_s} (1 - x_3)] E_a(t_a^{(1)}) S_t(x_3) h_a(\overline{(1 - r_{D_s}^2)x_2}, \overline{(1 - r_{D_{s_0}^*}^2)x_3}, b_2, b_3) \right. \\
&\quad \left. + [2r_{D_s} + r_{D_{s_0}^*} (1 - x_2)] E_a(t_a^{(2)}) S_t(x_2) h_a(\overline{(1 - r_{D_{s_0}^*}^2)x_3}, \overline{(1 - r_{D_s}^2)x_2}, b_3, b_2) \right\}, \tag{33}
\end{aligned}$$

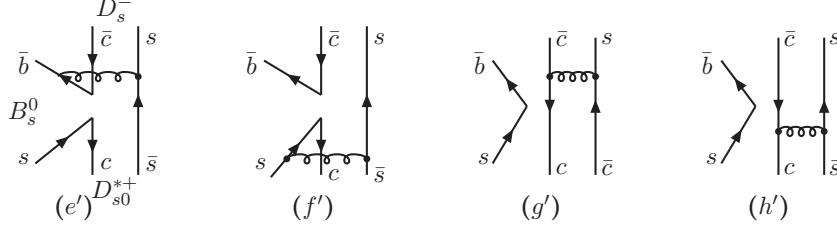


FIG. 2: Another part of diagrams contributing to the $B_s^0 \rightarrow D_{s0}^{*+}(2317)D_s^-$ decay.

where $\overline{(1 - r_{D_s}^2)x_2} = 1 - (1 - r_{D_s}^2)x_2$, $\overline{(1 - r_{D_{s0}^*}^2)x_3} = 1 - (1 - r_{D_{s0}^*}^2)x_3$. The hard scales, evolution factors, the expressions of the Sudakov factors and the functions of the hard kernels in the above amplitudes can be found in appendix A.

Another type of annihilation Feynman diagrams contributing to the decay $B_s \rightarrow D_{s0}^{*+}(2317)D_s^-$ are shown in Fig.2, and the corresponding amplitudes are written as

$$\begin{aligned} \mathcal{M}_{ancs}^{LL} &= -32\pi C_f m_{B_s}^4 / \sqrt{2N_C} \int_0^1 dx_1 dx_2 dx_3 \int_0^\infty b_1 db_1 b_2 db_2 \phi_{B_s}(x_1, b_1) \phi_{D_{s0}^*}(x_2) \phi_{D_s}(x_3) \\ &\quad \times \left\{ [x_3 - r_{D_s} r_{D_{s0}^*} (x_2 + x_3 + 2)] E_{an}(t_{ancs}^{(1)}) h_{ancs}^{(1)}(x_1, x_3, x_2, b_1, b_2) \right. \\ &\quad \left. - [x_2 - r_{D_s} r_{D_{s0}^*} (x_2 + x_3)] E_{an}(t_{ancs}^{(2)}) h_{ancs}^{(2)}(x_1, x_3, x_2, b_1, b_2) \right\}, \end{aligned} \quad (34)$$

$$\begin{aligned} \mathcal{M}_{ancs}^{LR} &= -32\pi C_f m_{B_s}^4 / \sqrt{2N_C} \int_0^1 dx_1 dx_2 dx_3 \int_0^\infty b_1 db_1 b_2 db_2 \phi_{B_s}(x_1, b_1) \phi_{D_{s0}^*}(x_2) \phi_{D_s}(x_3) \\ &\quad \times \left\{ [r_{D_s} (2 - x_3) - r_{D_{s0}^*} (x_2 - 2)] E_{an}(t_{ancs}^{(1)}) h_{ancs}^{(1)}(x_1, x_3, x_2, b_1, b_2) \right. \\ &\quad \left. + [r_{D_{s0}^*} x_2 + r_{D_s} x_3] E_{an}(t_{ancs}^{(2)}) h_{ancs}^{(2)}(x_1, x_3, x_2, b_1, b_2) \right\}, \end{aligned} \quad (35)$$

$$\begin{aligned} \mathcal{M}_{ancs}^{SP} &= 32\pi C_f m_{B_s}^4 / \sqrt{2N_C} \int_0^1 dx_1 dx_2 dx_3 \int_0^\infty b_1 db_1 b_2 db_2 \phi_{B_s}(x_1, b_1) \phi_{D_{s0}^*}(x_2) \phi_{D_s}(x_3) \\ &\quad \times \left\{ [x_2 - r_{D_s} r_{D_{s0}^*} (x_2 + x_3 + 2)] E_{an}(t_{ancs}^{(1)}) h_{ancs}^{(1)}(x_1, x_3, x_2, b_1, b_2) \right. \\ &\quad \left. - [x_3 - r_{D_s} r_{D_{s0}^*} (x_2 + x_3)] E_{an}(t_{ancs}^{(2)}) h_{ancs}^{(2)}(x_1, x_3, x_2, b_1, b_2) \right\}, \end{aligned} \quad (36)$$

$$\begin{aligned} \mathcal{F}_{acs}^{LL} &= -\mathcal{F}_{acs}^{LR} = -8\pi C_f f_{B_s} m_{B_s}^4 \int_0^1 dx_2 dx_3 \int_0^\infty b_2 db_2 b_3 db_3 \phi_{D_{s0}^*}(x_2) \phi_{D_s}(x_3) \\ &\quad \left\{ [1 - x_2 + 2r_{D_s} r_{D_{s0}^*} (x_2 - 2)] E_a(t_{acs}^{(1)}) S_t(x_2) h_a(x_3, (1 - r_{D_{s0}^*}^2 - r_{D_s}^2)x_2, b_3, b_2) \right. \\ &\quad \left. - [1 - x_3 + 2r_{D_s} r_{D_{s0}^*} (x_3 - 2)] E_a(t_{acs}^{(2)}) S_t(x_3) h_a(x_2, (1 - r_{D_{s0}^*}^2 - r_{D_s}^2)x_3, b_2, b_3) \right\}, \end{aligned} \quad (37)$$

$$\begin{aligned} \mathcal{F}_{acs}^{SP} &= 16\pi C_f f_{B_s} m_{B_s}^4 \int_0^1 dx_2 dx_3 \int_0^\infty b_2 db_2 b_3 db_3 \phi_{D_{s0}^*}(x_2) \phi_{D_s}(x_3) \\ &\quad \left\{ [-2r_{D_s} + r_{D_{s0}^*} (1 - x_2) + r_c] E_a(t_{acs}^{(1)}) S_t(x_2) h_a(x_3, (1 - r_{D_{s0}^*}^2 - r_{D_s}^2)x_2, b_3, b_2) \right. \\ &\quad \left. + [2r_{D_{s0}^*} - r_{D_s} (1 - x_3) - r_c] E_a(t_{acs}^{(2)}) S_t(x_3) h_a(x_2, (1 - r_{D_{s0}^*}^2 - r_{D_s}^2)x_3, b_2, b_3) \right\}. \end{aligned} \quad (38)$$

The amplitudes for the decay $B_s \rightarrow D_{s_0}^{*-} D_s^+$ are listed in Appendix B. As to the decays with a vector meson $D_{(s)}^*$ involved, the corresponding amplitudes can be also obtained from the Feymann rules, which are not listed for simplicity. Combining these amplitudes, we can obtain the total decay amplitude of each considered channel

$$\begin{aligned} \mathcal{A}(B^+ \rightarrow D_{s_0}^{*+} D^0) &= \frac{G_F}{\sqrt{2}} \left\{ V_{cb}^* V_{cs} [F_e^{LL}(a_1) + M_{en}^{LL}(C_1)] + V_{ub} V_{us} [F_a^{LL}(a_1) + M_{an}^{LL}(C_1)] \right. \\ &\quad - V_{tb}^* V_{ts} [F_e^{LL}(a_4 + a_{10}) + M_{en}^{LL}(C_3 + c_9) + F_e^{SP}(a_6 + a_8) \\ &\quad + M_{en}^{LR}(C_5 + C_7) + F_a^{LL}(a_4 + a_{10}) + F_a^{SP}(a_6 + a_8) \\ &\quad \left. + M_{an}^{LL}(C_3 + C_9) + M_{an}^{LR}(C_5 + C_7)] \right\}, \end{aligned} \quad (39)$$

$$\begin{aligned} \mathcal{A}(B^0 \rightarrow D_{s_0}^{*+} D^-) &= \frac{G_F}{\sqrt{2}} \left\{ V_{cb}^* V_{cs} [F_e^{LL}(a_1) + M_{en}^{LL}(C_1)] - V_{tb}^* V_{ts} [F_e^{LL}(a_4 + a_{10}) \right. \\ &\quad + F_e^{SP}(a_6 + a_8) + M_{en}^{LL}(C_3 + C_9) + M_{en}^{LR}(C_5 + C_7) + F_a^{LL}(a_4 - \frac{a_{10}}{2}) \\ &\quad \left. + F_a^{SP}(a_6 - \frac{a_8}{2}) + M_{an}^{LL}(C_3 - \frac{C_9}{2}) + M_{an}^{LR}(C_5 - \frac{C_7}{2}) \right\}, \end{aligned} \quad (40)$$

$$\begin{aligned} \mathcal{A}(B_s^0 \rightarrow D_{s_0}^{*+} D_s^-) &= \frac{G_F}{\sqrt{2}} \left\{ V_{cb}^* V_{cs} [F_e^{LL}(a_1) + M_{en}^{LL}(C_1) + F_{acs}^{LL}(a_2) + M_{ancs}^{LL}(C_2)] - V_{tb}^* V_{ts} [\right. \\ &\quad F_e^{LL}(a_4 + a_{10}) + F_e^{SP}(a_6 + a_8) + M_{en}^{LL}(C_3 + C_9) + M_{en}^{LR}(C_5 + C_7) \\ &\quad + F_{acs}^{LL}(a_3 - a_5 - a_7 + a_9) + M_{ancs}^{LL}(C_4 + C_{10}) + M_{ancs}^{SP}(C_6 + C_8) \\ &\quad + F_a^{LL}(a_3 + a_4 - a_5 + \frac{a_7}{2} - \frac{a_9}{2} - \frac{a_{10}}{2}) + M_{an}^{LL}(C_3 + C_4 - \frac{C_9}{2} - \frac{10}{2}) \\ &\quad \left. + F_a^{SP}(a_6 - \frac{a_8}{2}) + M_{an}^{SP}(C_6 - \frac{C_8}{2}) + M_{an}^{LR}(C_5 - \frac{C_7}{2}) \right\}, \end{aligned} \quad (41)$$

$$\begin{aligned} \mathcal{A}(B_s^0 \rightarrow D_{s_0}^{*-} D^+) &= \frac{G_F}{\sqrt{2}} \left\{ V_{cb}^* V_{cd} [F_{ec}^{LL}(a_1) + M_{enc}^{LL}(C_1)] - V_{tb}^* V_{td} [F_{ec}^{LL}(a_4 + a_{10}) \right. \\ &\quad + M_{enc}^{LL}(C_3 + C_9) + M_{enc}^{LR}(C_5 + C_7) + F_{ec}^{SP}(a_6 + a_8) + F_{ac}^{LL}(a_4 - \frac{a_{10}}{2}) \\ &\quad \left. + M_{anc}^{LL}(C_3 - \frac{C_9}{2}) + F_{ac}^{SP}(a_6 - \frac{a_8}{2}) + M_{anc}^{LR}(C_5 - \frac{C_7}{2}) \right\}. \end{aligned} \quad (42)$$

The amplitudes for the decay $B_s^0 \rightarrow D_{s_0}^{*-} D_s^+$ can be obtained from those for the decay $B_s^0 \rightarrow D_{s_0}^{*+} D_s^-$ by deleting (adding) the character "c" from (to) the subscript of each amplitude where there is (not) a character "c".

III. THE NUMERICAL RESULTS AND DISCUSSIONS

We use the following input parameters in the numerical calculations [6, 57]:

$$f_B = 210 \text{ MeV}, f_{B_s} = 230 \text{ MeV}, M_B = 5.28 \text{ GeV}, M_{B_s} = 5.37 \text{ GeV}, \quad (43)$$

$$\tau_B^\pm = 1.638 \times 10^{-12} \text{ s}, \tau_{B^0} = 1.519 \times 10^{-12} \text{ s}, \tau_{B_s} = 1.512 \times 10^{-12} \text{ s}, \quad (44)$$

$$M_W = 80.38 \text{ GeV}, M_{D_{s_0}^*} = 2.3178 \text{ GeV}. \quad (45)$$

TABLE II: Branching ratios ($\times 10^{-4}$) of the decays $B^+ \rightarrow D_{s_0}^{*+}(2317)\bar{D}^{(*)0}$ and $B^0 \rightarrow D_{s_0}^{*+}(2317)D^{(*)-}$ with different values $f_{D_{s_0}^*} = 55, 60, 67$ MeV, where the errors for these entries correspond to the uncertainties in the $w_b = 0.4 \pm 0.04$ GeV for B meson, the hard scale t varying from $0.75t$ to $1.25t$, and the CKM matrix elements.

Modes	$f_{D_{s_0}^*} = 55$	$f_{D_{s_0}^*} = 60$	$f_{D_{s_0}^*} = 67$	Data [6]
$Br(B^+ \rightarrow D_{s_0}^{*+}(2317)\bar{D}^0)$	$7.5^{+3.3+0.1+0.3}_{-2.2-0.3-0.3}$	$8.9^{+4.0+0.5+0.4}_{-2.6-0.2-0.3}$	$11.2^{+4.0+0.3+0.4}_{-2.8-0.2-0.4}$	$8.0^{+1.6}_{-1.3}$
$Br(B^+ \rightarrow D_{s_0}^{*+}(2317)\bar{D}^{*0})$	$12.0^{+4.9+1.9+0.5}_{-3.5-1.2-0.4}$	$14.4^{+6.0+2.3+0.5}_{-4.3-1.5-0.4}$	$18.3^{+7.1+2.7+0.7}_{-5.4-1.7-0.5}$	9 ± 7
$Br(B^0 \rightarrow D_{s_0}^{*+}(2317)D^-)$	$7.0^{+3.0+0.1+0.2}_{-2.1-0.2-0.3}$	$8.3^{+3.7+0.4+0.3}_{-2.4-0.2-0.3}$	$10.5^{+4.5+0.4+0.4}_{-3.0-0.2+0.4}$	10.6 ± 1.6
$Br(B^0 \rightarrow D_{s_0}^{*+}(2317)D^{*-})$	$10.5^{+4.7+1.6+0.3}_{-3.2-0.9-0.4}$	$12.6^{+5.7+1.9+0.5}_{-3.8-1.1-0.5}$	$15.9^{+7.0+2.4+0.6}_{-4.9-1.4-0.5}$	15 ± 6

For the CKM matrix elements, we adopt the Wolfenstein parametrization and the updated values $A = 0.790^{+0.017}_{-0.012}$, $\lambda = 0.22650 \pm 0.00048$, $\bar{\rho} = 0.141^{+0.016}_{-0.017}$ and $\bar{\eta} = 0.357 \pm 0.011$ [6].

Generally speaking that the branching ratio of the charged channel should not be less than that of the corresponding neutral one. For example, Particle Data Group(PDG) gives that $Br(B^+ \rightarrow D_s^+\bar{D}^0) = (9.0 \pm 0.9) \times 10^{-3}$, which is larger than $Br(B^0 \rightarrow D_s^+D^-) = (7.2 \pm 0.8) \times 10^{-3}$ [6]. Similarly our calculations (given in Table II) also show that the branching ratio of the charged decay $B^+ \rightarrow D_s^+(2317)\bar{D}^{(*)0}$ is slightly larger than that of the neutral decay $B^0 \rightarrow D_s^+(2317)D^{(*)-}$. But data are just opposite [6]. Certainly, there still exist large errors in the experimental results, especially for the branching ratios of the decays with a vector meson D^* involved. We expect more accurate experimental results in the future LHCb and Super KEKB experiments. Theoretically, the decays $B^+ \rightarrow D_s^+(2317)\bar{D}^{(*)0}$ and $B^0 \rightarrow D_s^+(2317)D^{(*)-}$ have the same CKM matrix elements and Wilson coefficients for the factorizable and nonfactorizable emission amplitudes, it is different in the amplitudes from the annihilation diagrams, while their contributions are small which will be discussed later. Furthermore, there exist similar transition form factors for isospin symmetry between each pair of decay channels. So they should have similar branching ratios.

Certainly, here most uncertainty parameter is the decay constant $f_{D_{s_0}^*}$, which is defined by the matrix element of the vector current

$$\langle 0 | \bar{s} \gamma_\mu c | D_{s_0}^*(\mathbf{p}) \rangle = f_{D_{s_0}^*} p_\mu. \quad (46)$$

It connects with another decay constant $\tilde{f}_{D_{s_0}^*}$ defined in Eq.(9) at zero momentum by the formula $f_{D_{s_0}^*} = \tilde{f}_{D_{s_0}^*} (m_c - m_s) / m_{D_{s_0}^*}$. The decay constant $f_{D_{s_0}^*}$ has been computed by different approaches with results covering a wide range (shown in Table I). It is interesting that the works [20–22, 62] about the analysis of the decay constant $f_{D_{s_0}^*}$ through B decays to two charmed mesons are consistent with each other: $f_{D_{s_0}^*}$ is in the range of $60 \sim 75$ MeV, which is much smaller than the decay constant of another P-wave meson $D_{s_1}(2460)$. That is to say that there exists large disparity between these two decay constants. And the corresponding analysis approaches include the heavy quark symmetry (HQS), the light front quark model (QM). While some authors considered that $f_{D_{s_0}^*}$ is larger than 100 MeV by using the quark model [15], lattice QCD (LQCD) [16] and so on.

From our calculations, we find that the smaller decay constant $f_{D_{s_0}^*}$ is supported by the present data, say $55 \sim 70$ MeV. The values such as larger than 100 MeV seem are

TABLE III: The ratios $R_{1,2}$ defined in Eq.(47) with different values $f_{D_{s_0}^*} = 55, 60, 67$ MeV, where the errors are the same with those in Tab.2, but with them added in quadrature.

Modes	$f_{D_{s_0}^*} = 55$	$f_{D_{s_0}^*} = 60$	$f_{D_{s_0}^*} = 67$	Data [6]
R_1	$0.63^{+0.39}_{-0.27}$	$0.62^{+0.40}_{-0.26}$	$0.61^{+0.33}_{-0.24}$	$0.89^{+0.71}_{-0.70}$
R_2	$0.67^{+0.43}_{-0.29}$	$0.66^{+0.43}_{-0.28}$	$0.66^{+0.42}_{-0.28}$	0.71 ± 0.30

not favored. So we calculate the branching ratios corresponding to $f_{D_{s_0}^*} = 55, 60, 67$ MeV and list in Table II.

It is helpful to define the following two ratios

$$R_1 = \frac{Br(B^+ \rightarrow D_{s_0}^{*+}(2317)\bar{D}^0)}{Br(B^+ \rightarrow D_{s_0}^{*+}(2317)\bar{D}^{*0})}, \quad R_2 = \frac{Br(B^0 \rightarrow D_{s_0}^{*+}(2317)D^-)}{Br(B^0 \rightarrow D_{s_0}^{*+}(2317)D^{*-})}. \quad (47)$$

They are in the range $0.61 \sim 0.67$ (shown in Table III), which are lower than the experimental values 0.89 and 0.71, respectively. Certainly, these two ratios can be well determined by the future experiments through improving the measurement accuracy to the decays $B^+ \rightarrow D_{s_0}^{*+}(2317)\bar{D}^{*0}$ and $B^0 \rightarrow D_{s_0}^{*+}(2317)D^{*-}$. It is very possible that the ratios R_1 and R_2 are less than 1, which is contrary to the previous prediction [62].

Here we take $B^0 \rightarrow D_{s_0}^{*+}(2317)D^-$ as an example to do the numerical analysis about the amplitudes from different types of Feynman diagrams. The tree operators from the factorizable emission diagrams give the largest contribution because of the large Wilson coefficient $C_2 + C_1/3$, and the value of the corresponding amplitude is about 4.39×10^{-2} . The amplitude from the nonfactorizable emission diagrams is suppressed by the small Wilson coefficient C_1 , whose value is about $(1.32 + i0.57) \times 10^{-2}$. The total amplitude of penguin operators is about $-(0.95 + i0.07) \times 10^{-2}$, which comes from two parts: One is the factorizable and nonfactorizable emission diagrams $-(0.93 + i0.04) \times 10^{-2}$, the other is the annihilation diagrams $-(1.11 + i3.67) \times 10^{-4}$. The penguin operators receive severe suppression from the Wilson coefficients and only contribute 3.9% to the final branching ratio. The penguin operator contributions from the annihilation diagrams are even tiny and can be neglected. So it is enough to pay our attention only to the factorizable and nonfactorizable emission diagrams for the investigation of the branching ratios. As to the branching ratios for the decays of B_s to two charmed mesons are also calculated and listed in Table IV. In these decays, $B_s \rightarrow D_{s_0}^{*-}(2317)D_s^{(*)+}$ have the largest branching ratios, which are at 10^{-3} order. They are consistent with the predictions by the relativistic quark model (RQM) [56], while are much smaller than those by using the light cone sum rules (LCSR) approach [51]. It can be tested by the future LHCb and Super KEKB experiments. For the decays $B_s \rightarrow D_{s_0}^{*-}(2317)D_s^{(*)+}$, their branching ratios are much smaller than other four channels mainly because of the smaller CKM matrix element V_{cd} compared with V_{cs} , that is to say there exists a suppressed factor $|V_{cd}/V_{cs}|^2 \approx 0.05$ between the branching ratios of these two types of decays.

Through our calculations, we find that the direct CP asymmetries of our considered decays are in the range of $10^{-4} \sim 10^{-3}$. For example, $A_{CP}^{dir}(B^+ \rightarrow D_{s_0}^+(2317)D^0)$ is about 0.75%. As we know that the direct CP asymmetry is proportional to the interference between the tree and penguin contributions, while the penguin contributions are small as

TABLE IV: Branching ratios ($\times 10^{-3}$) of the decays $B_s \rightarrow D_{s0}^*(2317)D_s^{(*)}$, $D_{s0}^*(2317)D^{(*)}$ with different values $f_{D_{s0}^*} = 55, 60, 67$ MeV, where the errors for these entries correspond to the uncertainties in the $w_b = 0.5 \pm 0.05$ GeV for B_s meson, the hard scale t varying from $0.75t$ to $1.25t$, and the CKM matrix elements. Some of these channels have been calculated by using the light cone sum rules (LCSR) [51] and the relativistic quark model (RQM) [56], which are listed in the last two columns.

Modes	$f_{D_{s0}^*} = 55\text{MeV}$	$f_{D_{s0}^*} = 60\text{MeV}$	$f_{D_{s0}^*} = 67\text{MeV}$	RQM [56]	LCSR [51]
$B_s \rightarrow D_{s0}^{*-}(2317)D_s^+$	$1.4^{+0.6+0.2+0.1}_{-0.4-0.1-0.0}$	$1.7^{+0.8+0.2+0.0}_{-0.5-0.1-0.1}$	$2.1^{+0.9+0.3+0.1}_{-0.6-0.1-0.1}$	1.1	13^{+7}_{-5}
$B_s \rightarrow D_{s0}^{*+}(2317)D_s^{*+}$	$1.2^{+0.5+0.1+0.0}_{-0.4-0.1-0.1}$	$1.4^{+0.8+0.1+0.1}_{-0.4-0.1-0.0}$	$1.8^{+0.9+0.1+0.1}_{-0.6-0.1-0.1}$	2.3	$6.0^{+2.9}_{-2.4}$
$B_s \rightarrow D_{s0}^{*-}(2317)D_s^-$	$0.73^{+0.35+0.02+0.03}_{-0.24-0.04-0.01}$	$0.86^{+0.56+0.04+0.03}_{-0.27-0.03-0.03}$	$1.11^{+0.56+0.02+0.04}_{-0.37-0.04-0.04}$		
$B_s \rightarrow D_{s0}^{*+}(2317)D_s^{*-}$	$0.97^{+0.45+0.07+0.03}_{-0.31-0.06-0.04}$	$1.17^{+0.56+0.08+0.04}_{-0.37-0.07-0.05}$	$1.48^{+0.69+0.05+0.06}_{-0.46-0.07-0.05}$		
$B_s \rightarrow D_{s0}^{*-}(2317)D^+$	$0.043^{+0.023+0.004+0.002}_{-0.014-0.003-0.001}$	$0.052^{+0.027+0.005+0.002}_{-0.017-0.003-0.002}$	$0.065^{+0.034+0.006+0.002}_{-0.021-0.004-0.002}$		$0.5^{+0.2}_{-0.2}$
$B_s \rightarrow D_{s0}^{*+}(2317)D^{*+}$	$0.033^{+0.018+0.003+0.001}_{-0.011-0.002-0.001}$	$0.040^{+0.021+0.003+0.001}_{-0.014-0.002-0.001}$	$0.050^{+0.026+0.004+0.002}_{-0.017-0.002-0.001}$		$0.2^{+0.1}_{-0.1}$

we mentioned above, so it is not surprise that the direct CP violation of these decays are small. In a word, the direct CP asymmetries in these decays of B to two charmed mesons are tiny, any large direct CP violation observed in the future experiments can be treated as a new dynamic mechanism from the some special structure of $D_{s0}^{*+}(2317)$ or a signal of new physics.

IV. CONCLUSION

In summary, we probe the inner structure of the meson $D_{s0}^*(2317)$ through the decays of $B_{(s)}$ to two charmed mesons within pQCD approach. Assuming $D_{s0}^*(2317)$ as a scalar meson with $\bar{c}s$ structure, we find that our predictions for the branching ratios of the decays $B^+ \rightarrow D_{s0}^{*+}(2317)\bar{D}^{(*)0}$, $B^0 \rightarrow D_{s0}^{*+}(2317)D^{(*)-}$ can explain data within errors. In our calculations, the decay constant of the meson $D_{s0}^*(2317)$ is an input parameter, and its value has been studied by many references but with results covering a wide range. While a smaller value of the decay constant for the meson $D_{s0}^*(2317)$ is supported in our work, say $55 \sim 70$ MeV. We also calculate the ratios $R_1 = \frac{Br(B^+ \rightarrow D_{s0}^{*+}(2317)\bar{D}^0)}{Br(B^+ \rightarrow D_{s0}^{*+}(2317)\bar{D}^{*0})}$ and $R_2 = \frac{Br(B^0 \rightarrow D_{s0}^{*+}(2317)D^-)}{Br(B^0 \rightarrow D_{s0}^{*+}(2317)D^{*-})}$, which are valuable to determine the inner structure of the meson $D_{s0}^*(2317)$ by compared between theory and experiment. We expect that these two values can be well measured by the future LHCb and Super KEKB experiments through improving the measurement accuracy for the decays $B^+ \rightarrow D_{s0}^{*+}(2317)\bar{D}^{*0}$ and $B^0 \rightarrow D_{s0}^{*+}(2317)D^{*-}$.

Acknowledgment

This work is supported by the National Natural Science Foundation of China under Grant No. 11347030, 11847097 and by the Program of Science and Technology Innovation Talents in Universities of Henan Province 14HASTIT037. One of us (N. Wang)

is supported by the Science Research Fund Project for the High-Level Talents of Henan University of Technology 004/31401151.

Appendix A: Scales, functions for the hard kernel and The evolution factors

The variables that are evaluated from the gluon and quark propagators will be used to determine the scales and the expressions of the hard kernels

$$P_{en} = m_B^2 x_1 x_3 (1 - r_{D_{s0}^*}^2), P_{en}^{(1)} = m_B^2 x_3 (x_1 (1 - r_{D_{s0}^*}^2) - x_2 (1 - r_{D_{s0}^*}^2 - r_{D_s}^2)), \quad (\text{A1})$$

$$P_{en}^{(2)} = m_B^2 \left[r_c^2 - ((1 - x_1 - x_2)x_3 - (1 - x_2)x_3 r_{D_s}^2 + (1 - x_1 - x_2)(1 - x_3)r_{D_{s0}^*}^2) \right], \quad (\text{A2})$$

$$P_{an} = -m_B^2 \left[1 - (1 - r_{D_s}^2)x_2 - (1 - r_{D_{s0}^*}^2)x_3 + x_2 x_3 (1 - r_{D_s}^2 - r_{D_{s0}^*}^2) \right], \quad (\text{A3})$$

$$P_{an}^{(1)} = m_B^2 \left[1 + (1 - r_{D_{s0}^*}^2)x_1 x_3 - (1 - r_{D_s}^2 - r_{D_{s0}^*}^2)x_2 x_3 \right], \quad (\text{A4})$$

$$P_{an}^{(2)} = m_B^2 \left[x_1 + x_2 + x_3 - 1 - x_1 x_3 (1 - r_{D_{s0}^*}^2) - x_2 r_D^2 - x_3 r_{D_{s0}^*}^2 - x_2 x_3 (1 - r_D^2 - r_{D_{s0}^*}^2) \right], \quad (\text{A5})$$

$$P_{ancs} = -m_B^2 \left(1 - r_{D_s}^2 - r_{D_{s0}^*}^2 \right) x_2 x_3, P_{ancs}^{(2)} = m_B^2 \left[x_1 (1 - r_{D_{s0}^*}^2) - (1 - r_{D_s}^2 - r_{D_{s0}^*}^2)x_2 \right] x_3, \quad (\text{A6})$$

$$P_{ancs}^{(1)} = m_B^2 \left[x_1 (1 + (r_{D_{s0}^*}^2 - 1)x_3) + x_3 (1 - r_{D_{s0}^*}^2) + x_2 (1 - x_3 (1 - r_{D_{s0}^*}^2) + (x_3 - 1)r_{D_s}^2) \right]. \quad (\text{A7})$$

Then the scales in each amplitude are determined as

$$t_e^{(1)} = \max(\sqrt{x_3 (1 - r_{D_{s0}^*}^2)} m_B, 1/b_1, 1/b_3), \quad (\text{A8})$$

$$t_e^{(2)} = \max(\sqrt{x_1 (1 - r_{D_{s0}^*}^2)} m_B, 1/b_1, 1/b_3), \quad (\text{A9})$$

$$t_{en}^{(1,2)} = \max(\sqrt{P_{en}}, \sqrt{|P_{en}^{(1,2)}|}, 1/b_1, 1/b_2), \quad (\text{A10})$$

$$t_{an}^{(1,2)} = \max(\sqrt{|P_{an}|}, \sqrt{|P_{an}^{(1,2)}|}, 1/b_1, 1/b_3), \quad (\text{A11})$$

$$t_{ancs}^{(1,2)} = \max(\sqrt{|P_{ancs}|}, \sqrt{|P_{ancs}^{(1,2)}|}, 1/b_1, 1/b_2), \quad (\text{A12})$$

$$t_a^{(1)} = \max(\sqrt{1 - (1 - r_{D_{s0}^*}^2)x_3}, 1/b_2, b_3), \quad (\text{A13})$$

$$t_a^{(2)} = \max(\sqrt{1 - (1 - r_{D_s}^2)x_2}, 1/b_2, b_3), \quad (\text{A14})$$

$$t_{acs}^{(1)} = \max(\sqrt{(1 - r_{D_s}^2 - r_{D_{s0}^*}^2)x_2}, 1/b_2, b_3), \quad (\text{A15})$$

$$t_{acs}^{(2)} = \max(\sqrt{(1 - r_{D_s}^2 - r_{D_{s0}^*}^2)x_3}, 1/b_2, b_3). \quad (\text{A16})$$

The hard functions for the hard part of the amplitudes are listed as

$$h_e(x_1, x_3, b_1, b_3) = K_0(\sqrt{x_1 x_3} m_{B_s} b_1) [\theta(b_1 - b_3) K_0(\sqrt{x_3} m_{B_s} b_1) I_0(\sqrt{x_3} m_{B_s} b_3) + \theta(b_3 - b_1) K_0(\sqrt{x_3} m_{B_s} b_3) I_0(\sqrt{x_3} m_{B_s} b_1)], \quad (\text{A17})$$

$$h_a(x_2, x_3, b_2, b_3) = \left(i\frac{\pi}{2}\right)^2 H_0^{(1)}(\sqrt{x_2 x_3} m_{B_s} b_2) \left[\theta(b_2 - b_3) H_0^{(1)}(\sqrt{x_3} m_{B_s} b_2) J_0(\sqrt{x_3} m_{B_s} b_3) + \theta(b_3 - b_2) H_0^{(1)}(\sqrt{x_3} m_{B_s} b_3) J_0(\sqrt{x_3} m_{B_s} b_2)\right], \quad (\text{A18})$$

$$h_{en}^{(j)}(x_1, x_2, x_3, b_1, b_2) = \left[\theta(b_1 - b_2) K_0(\sqrt{P_{en}} b_1) I_0(\sqrt{P_{en}} b_2) + (b_1 \leftrightarrow b_2)\right] \begin{pmatrix} K_0(\sqrt{P_{en}^{(j)}} b_2) & \text{for } P_{en}^{(j)} \geq 0 \\ \frac{i\pi}{2} H_0^{(1)}(\sqrt{|P_{en}^{(j)}}| b_2) & \text{for } P_{en}^{(j)} \leq 0 \end{pmatrix}, \quad (\text{A19})$$

$$h_{an(cs)}^{(j)}(x_1, x_2, x_3, b_1, b_3) = i\frac{\pi}{2} \left[\theta(b_1 - b_3) H_0^{(1)}(\sqrt{P_{an(cs)}} b_1) J_0(\sqrt{P_{an(cs)}} b_3) + (b_1 \leftrightarrow b_3)\right] \begin{pmatrix} K_0(\sqrt{P_{an(cs)}^{(j)}} b_1) & \text{for } P_{an(cs)}^{(j)} \geq 0 \\ \frac{i\pi}{2} H_0^{(1)}(\sqrt{|P_{an(cs)}^{(j)}}| b_1) & \text{for } P_{an(cs)}^{(j)} \leq 0 \end{pmatrix}, \quad (\text{A20})$$

where the functions $H_0^{(1)}$, J_0 , K_0 , I_0 are the (modified) Bessel functions and obtained from the Fourier transformations of the quark and gluon propagators. The evolution factors evolving the scale t are defined as

$$E_e(t) = \alpha_s(t) \exp[-S_{B_s}(t) - S_{D_s}(t)], \quad (\text{A21})$$

$$E_{en}(t) = \alpha_s(t) \exp[-S_{B_s}(t) - S_{D_s}(t) - S_{D_{s0}^*}(t)|_{b_1=b_3}], \quad (\text{A22})$$

$$E_{an}(t) = \alpha_s(t) \exp[-S_{B_s}(t) - S_{D_s}(t) - S_{D_{s0}^*}(t)|_{b_2=b_3}], \quad (\text{A23})$$

$$E_a(t) = \alpha_s(t) \exp[-S_{D_s}(t) - S_{D_{s0}^*}(t)], \quad (\text{A24})$$

where the definitions of the functions $S_j(t)$ ($j = B_s, D_{D_{s0}^*}, D_s$) in Eq.(A21), Eq.(A22), Eq.(A23) and Eq.(A24) are given as

$$S_{B_s}(t) = s(x_1 \frac{m_{B_s}}{\sqrt{2}}, b_1) + \frac{5}{3} \int_{1/b_1}^t \frac{d\bar{\mu}}{\bar{\mu}} \gamma_q(\alpha_s(\bar{\mu})), \quad (\text{A25})$$

$$S_{D_s}(t) = s(x_2 \frac{m_{B_s}}{\sqrt{2}}, b_2) + 2 \int_{1/b_2}^t \frac{d\bar{\mu}}{\bar{\mu}} \gamma_q(\alpha_s(\bar{\mu})), \quad (\text{A26})$$

$$S_{D_{s0}^*}(t) = s(x_3 \frac{m_{B_s}}{\sqrt{2}}, b_3) + 2 \int_{1/b_3}^t \frac{d\bar{\mu}}{\bar{\mu}} \gamma_q(\alpha_s(\bar{\mu})). \quad (\text{A27})$$

Here the quark anomalous dimension $\gamma_q = -\alpha_s/\pi$, and the expression of the $s(Q, b)$ in one-loop running coupling constant is used

$$s(Q, b) = \frac{A^{(1)}}{2\beta_1} \hat{q} \ln\left(\frac{\hat{q}}{\hat{b}}\right) - \frac{A^{(1)}}{2\beta_1} (\hat{q} - \hat{b}) + \frac{A^{(2)}}{4\beta_1^2} \left(\frac{\hat{q}}{\hat{b}} - 1\right) - \left[\frac{A^{(2)}}{4\beta_1^2} - \frac{A^{(1)}}{4\beta_1} \ln\left(\frac{e^{2\gamma_E - 1}}{2}\right)\right] \ln\left(\frac{\hat{q}}{\hat{b}}\right), \quad (\text{A28})$$

with the variables are defined by $\hat{q} = \ln[Q/(\sqrt{2}\Lambda)]$, $\hat{q} = \ln[1/(b\Lambda)]$ and the coefficients $A^{(1,2)}$ and β_1 are

$$\beta_1 = \frac{33 - 2n_f}{12}, A^{(1)} = \frac{4}{3}, \quad (\text{A29})$$

$$A^{(2)} = \frac{67}{9} - \frac{\pi^2}{3} - \frac{10}{27}n_f + \frac{8}{3}\beta_1 \ln\left(\frac{1}{2}e^{\gamma_E}\right), \quad (\text{A30})$$

where n_f is the number of the quark flavors and γ_E the Euler constant.

Appendix B: Amplitudes for the decay $B_s^0 \rightarrow D_{s0}^{*-}(2317)D_s^+$

The amplitudes for the decay $B_s^0 \rightarrow D_{s0}^{*-}(2317)D_s^+$ are listed in the following. It is noticed that we add the character "c" in the subscripts to distinguish them from those for Fig.1, which represents a conventional charmed meson D_s being the emission (upper) position in the Feynman diagrams.

$$\begin{aligned} \mathcal{F}_{ec}^{LL} &= -\mathcal{F}_{ec}^{LR} = 8\pi C_F M_{B_s}^4 f_{D_s} \int_0^1 dx_1 dx_2 \int_0^\infty b_1 db_1 b_2 db_2 \phi_{B_s}(x_1, b_1) \phi_{D_{s0}^*}(x_2) \\ &\times [1 + r_{D_{s0}^*} + (1 - 2r_{D_{s0}^*})x_2] E_{ec}(t_{ec}^{(1)}) S_t(x_2) h_e(x_1, x_2(1 - r_{D_s}^2), b_1, b_2) \\ &+ [r_c(1 - 2r_{D_{s0}^*}) + r_{D_{s0}^*}(2 - r_{D_{s0}^*})] E_{ec}(t_{ec}^{(2)}) S_t(x_1) h_e(x_2, x_1(1 - r_{D_s}^2), b_2, b_1)], \quad (\text{B1}) \end{aligned}$$

$$\begin{aligned} \mathcal{F}_{ec}^{SP} &= -16\pi C_F M_{B_s}^4 f_{D_s} r_{D_s} \int_0^1 dx_1 dx_2 \int_0^\infty b_1 db_1 b_2 db_2 \phi_{B_s}(x_1, b_1) \\ &\times \{ [1 + r_{D_{s0}^*}(2 + r_{D_{s0}^*} + x_2(1 - 4r_{D_{s0}^*}))] E_{ec}(t_{ec}^{(1)}) S_t(x_2) h_e(x_1, x_2(1 - r_{D_s}^2), b_1, b_2) \\ &+ [r_c(1 - 4r_{D_{s0}^*}) + 2r_{D_{s0}^*}(1 - r_{D_{s0}^*})] E_{ec}(t_{ec}^{(2)}) S_t(x_1) h_e(x_2, x_1(1 - r_{D_s}^2), b_2, b_1) \}, \quad (\text{B2}) \end{aligned}$$

$$\begin{aligned} \mathcal{M}_{enc}^{LL} &= 32\pi C_f m_{B_s}^4 / \sqrt{2N_C} \int_0^1 dx_1 dx_2 dx_3 \int_0^\infty b_1 db_1 b_3 db_3 \phi_{B_s}(x_1, b_1) \phi_{D_{s0}^*}(x_2) \phi_{D_s}(x_3) \\ &\times \{ [x_3 - r_{D_{s0}^*} x_2(1 - 2r_{D_{s0}^*})] E_{enc}(t_{enc}^{(1)}) h_{enc}^{(1)}(x_1, x_3, x_2, b_1, b_3) \\ &+ [x_3 - 1 - (1 - r_{D_{s0}^*})x_2 + r_c r_D] E_{enc}(t_{enc}^{(2)}) h_{enc}^{(2)}(x_1, x_3, x_2, b_1, b_3) \}, \quad (\text{B3}) \end{aligned}$$

$$\begin{aligned} \mathcal{M}_{enc}^{LR} &= -32\pi C_f m_{B_s}^4 / \sqrt{2N_C} \int_0^1 dx_1 dx_2 dx_3 \int_0^\infty b_1 db_1 b_3 db_3 \phi_{B_s}(x_1, b_1) \phi_{D_{s0}^*}(x_2) \phi_{D_s}(x_3) \\ &\times (r_{D_{s0}^*} + 1) \{ r_{D_s} [x_3 + r_{D_{s0}^*}(1 + r_{D_{s0}^*})x_2] E_{enc}(t_{enc}^{(1)}) h_{enc}^{(1)}(x_1, x_3, x_2, b_1, b_3) \\ &- [r_c + r_{D_s}(1 + r_{D_{s0}^*})(1 - x_3)] E_{enc}(t_{enc}^{(2)}) h_{enc}^{(2)}(x_1, x_3, x_2, b_1, b_3) \}, \quad (\text{B4}) \end{aligned}$$

$$\begin{aligned} \mathcal{M}_{enc}^{SP} &= -32\pi C_f m_{B_s}^4 / \sqrt{2N_C} \int_0^1 dx_1 dx_2 dx_3 \int_0^\infty b_1 db_1 b_3 db_3 \phi_{B_s}(x_1, b_1) \phi_{D_{s0}^*}(x_2) \phi_{D_s}(x_3) \\ &\times \{ [x_3 + (1 - r_{D_{s0}^*})x_2] E_{enc}(t_{enc}^{(1)}) h_{enc}^{(1)}(x_1, x_3, x_2, b_1, b_3) \\ &+ [x_3 + r_{D_{s0}^*} x_2 - 1] E_{enc}(t_{enc}^{(2)}) h_{enc}^{(2)}(x_1, x_3, x_2, b_1, b_3) \}, \quad (\text{B5}) \end{aligned}$$

where these amplitudes are factorizable and nonfactorizable emission contributions, respectively. The nonfactorizable and factorizable annihilation amplitudes are written as

$$\begin{aligned} \mathcal{M}_{anc}^{LL} &= 32\pi C_f m_{B_s}^4 / \sqrt{2N_C} \int_0^1 dx_1 dx_2 dx_3 \int_0^\infty b_1 db_1 b_2 db_2 \phi_{B_s}(x_1, b_1) \phi_{D_{s0}^*}(x_2) \phi_{D_s}(x_3) \\ &\quad \times \left\{ [x_3 - 1 - r_{D_s} r_{D_{s0}^*}(x_2 + x_3 - 4)] E_{an}(t_{anc}^{(1)}) h_{anc}^{(1)}(x_1, x_3, x_2, b_1, b_2) \right. \\ &\quad \left. + [1 - x_2 + r_{D_s} r_{D_{s0}^*}(x_2 + x_3 - 2)] E_{an}(t_{anc}^{(2)}) h_{anc}^{(2)}(x_1, x_3, x_2, b_1, b_2) \right\}, \end{aligned} \quad (\text{B6})$$

$$\begin{aligned} \mathcal{M}_{anc}^{LR} &= -32\pi C_f m_B^4 / \sqrt{2N_C} \int_0^1 dx_1 dx_2 dx_3 \int_0^\infty b_1 db_1 b_2 db_2 \phi_{B_s}(x_1, b_1) \phi_{D_{s0}^*}(x_2) \phi_{D_s}(x_3) \\ &\quad \times \left\{ [r_{D_s}(1 + x_3) + r_{D_{s0}^*}(1 + x_2)] E_{an}(t_{anc}^{(1)}) h_{anc}^{(1)}(x_1, x_3, x_2, b_1, b_2) \right. \\ &\quad \left. + [r_{D_{s0}^*}(1 - x_2) + r_{D_s}(1 - x_3)] E_{an}(t_{anc}^{(2)}) h_{anc}^{(2)}(x_1, x_3, x_2, b_1, b_2) \right\}, \end{aligned} \quad (\text{B7})$$

$$\begin{aligned} \mathcal{M}_{anc}^{SP} &= 32\pi C_f m_B^4 / \sqrt{2N_C} \int_0^1 dx_1 dx_2 dx_3 \int_0^\infty b_1 db_1 b_2 db_2 \phi_{B_s}(x_1, b_1) \phi_{D_{s0}^*}(x_2) \phi_{D_s}(x_3) \\ &\quad \times \left\{ [1 - x_2 + r_{D_s} r_{D_{s0}^*}(x_2 + x_3 - 4)] E_{an}(t_{anc}^{(1)}) h_{anc}^{(1)}(x_1, x_3, x_2, b_1, b_2) \right. \\ &\quad \left. - [1 - x_3 + r_{D_s} r_{D_{s0}^*}(x_2 + x_3 - 2)] E_{an}(t_{anc}^{(2)}) h_{anc}^{(2)}(x_1, x_3, x_2, b_1, b_2) \right\}, \end{aligned} \quad (\text{B8})$$

$$\begin{aligned} \mathcal{F}_{ac}^{LL} &= -\mathcal{F}_{ac}^{LR} = 8\pi C_f f_{B_s} m_{B_s}^4 \int_0^1 dx_2 dx_3 \int_0^\infty b_2 db_2 b_3 db_3 \phi_{D_{s0}^*}(x_2) \phi_{D_s}(x_3) \\ &\quad \left\{ [x_2 - 1 - 2r_{D_s} r_{D_{s0}^*}(x_2 - 2)] E_a(t_{ac}^{(1)}) S_t(x_2) h_a(\overline{(1 - r_{D_{s0}^*}^2)x_3}, \overline{(1 - r_{D_s}^2)x_2}, b_3, b_2) \right. \\ &\quad \left. + [1 - x_3 + 2r_{D_s} r_{D_{s0}^*}(x_3 - 2)] E_a(t_{ac}^{(2)}) S_t(x_3) h_a(\overline{(1 - r_{D_s}^2)x_2}, \overline{(1 - r_{D_{s0}^*}^2)x_3}, b_2, b_3) \right\}, \end{aligned} \quad (\text{B9})$$

$$\begin{aligned} \mathcal{F}_{ac}^{SP} &= 16\pi C_f f_{B_s} m_{B_s}^4 \int_0^1 dx_2 dx_3 \int_0^\infty b_2 db_2 b_3 db_3 \phi_{D_{s0}^*}(x_2) \phi_{D_s}(x_3) \\ &\quad \left\{ [-2r_{D_s} + r_{D_{s0}^*}(1 - x_2)] E_a(t_{ac}^{(1)}) S_t(x_2) h_a(\overline{(1 - r_{D_{s0}^*}^2)x_3}, \overline{(1 - r_{D_s}^2)x_2}, b_3, b_2) \right. \\ &\quad \left. + [2r_{D_{s0}^*} - r_{D_s}(1 - x_3)] E_a(t_{ac}^{(2)}) S_t(x_3) h_a(\overline{(1 - r_{D_s}^2)x_2}, \overline{(1 - r_{D_{s0}^*}^2)x_3}, b_2, b_3) \right\}. \end{aligned} \quad (\text{B10})$$

If changing the the positions of the scalar and the pseudoscalar mesons in the final states, one can get another type of annihilation amplitudes, which are given as

$$\begin{aligned} \mathcal{M}_{ans}^{LL} &= -32\pi C_f m_{B_s}^4 / \sqrt{2N_C} \int_0^1 dx_1 dx_2 dx_3 \int_0^\infty b_1 db_1 b_3 db_3 \phi_{B_s}(x_1, b_1) \phi_{D_{s0}^*}(x_2) \phi_{D_s}(x_3) \\ &\quad \times \left\{ [x_2 + r_{D_s} r_{D_{s0}^*}(x_2 + x_3 + 2)] E_{an}(t_{ans}^{(1)}) h_{ans}^{(1)}(x_1, x_2, x_3, b_1, b_3) \right. \\ &\quad \left. - [x_3 + r_{D_s} r_{D_{s0}^*}(x_2 + x_3)] E_{an}(t_{ans}^{(2)}) h_{ans}^{(2)}(x_1, x_3, x_2, b_1, b_3) \right\}, \end{aligned} \quad (\text{B11})$$

$$\begin{aligned} \mathcal{M}_{ans}^{LR} &= -32\pi C_f m_{B_s}^4 / \sqrt{2N_C} \int_0^1 dx_1 dx_2 dx_3 \int_0^\infty b_1 db_1 b_3 db_3 \phi_{B_s}(x_1, b_1) \phi_{D_{s0}^*}(x_2) \phi_{D_s}(x_3) \\ &\quad \times \left\{ [r_{D_s}(2 - x_3) + r_{D_{s0}^*}(x_2 - 2)] E_{an}(t_{ans}^{(1)}) h_{ans}^{(1)}(x_1, x_2, x_3, b_1, b_3) \right. \\ &\quad \left. - [r_{D_{s0}^*} x_2 - r_{D_s} x_3] E_{an}(t_{ans}^{(2)}) h_{ans}^{(2)}(x_1, x_2, x_3, b_1, b_3) \right\}, \end{aligned} \quad (\text{B12})$$

$$\begin{aligned}
\mathcal{M}_{ans}^{SP} &= 32\pi C_f m_{B_s}^4 / \sqrt{2N_C} \int_0^1 dx_1 dx_2 dx_3 \int_0^\infty b_1 db_1 b_3 db_3 \phi_{B_s}(x_1, b_1) \phi_{D_{s_0}^*}(x_2) \phi_{D_s}(x_3) \\
&\times \left\{ [x_3 + r_{D_s} r_{D_{s_0}^*}(x_2 + x_3 + 2)] E_{an}(t_{ans}^{(1)}) h_{ans}^{(1)}(x_1, x_2, x_3, b_1, b_3) \right. \\
&\left. - [x_2 + r_{D_s} r_{D_{s_0}^*}(x_2 + x_3)] E_{an}(t_{ans}^{(2)}) h_{ans}^{(2)}(x_1, x_2, x_3, b_1, b_3) \right\}, \tag{B13}
\end{aligned}$$

$$\begin{aligned}
\mathcal{F}_{as}^{LL} &= -\mathcal{F}_{as}^{LR} = -8\pi C_f f_{B_s} m_{B_s}^4 \int_0^1 dx_2 dx_3 \int_0^\infty b_2 db_2 b_3 db_3 \phi_{D_{s_0}^*}(x_2) \phi_{D_s}(x_3) \\
&\left\{ [x_3 + 2r_{D_s} r_{D_{s_0}^*}(1 + x_3)] E_a(t_{as}^{(1)}) S_t(x_3) h_a(x_2, (1 - r_{D_{s_0}^*}^2 - r_{D_s}^2)x_3, b_2, b_3) \right. \\
&\left. - [x_2 + 2r_{D_s} r_{D_{s_0}^*}(x_2 + 1)] E_a(t_{as}^{(2)}) S_t(x_2) h_a(x_3, (1 - r_{D_{s_0}^*}^2 - r_{D_s}^2)x_2, b_3, b_2) \right\}, \tag{B14}
\end{aligned}$$

$$\begin{aligned}
\mathcal{F}_{as}^{SP} &= 16\pi C_f f_{B_s} m_{B_s}^4 \int_0^1 dx_2 dx_3 \int_0^\infty b_2 db_2 b_3 db_3 \phi_{D_{s_0}^*}(x_2) \phi_{D_s}(x_3) \\
&\left\{ [2r_{D_{s_0}^*} + r_{D_s} x_3 + r_c] E_a(t_{as}^{(1)}) S_t(x_3) h_a(x_2, (1 - r_{D_{s_0}^*}^2 - r_{D_s}^2)x_3, b_2, b_3) \right. \\
&\left. + [2r_{D_s} + r_{D_{s_0}^*} x_2 - r_c] E_a(t_{as}^{(2)}) S_t(x_2) h_a(x_3, (1 - r_{D_{s_0}^*}^2 - r_{D_s}^2)x_2, b_2, b_3) \right\}. \tag{B15}
\end{aligned}$$

From the previews contents, it is easy to know that the character "s" in each subscript represents $s\bar{s}$ pair generated from a hard gluon in the corresponding Feynman diagrams. The scales, the functions for the hard kernel and the evolution factors can be obtained for Eq.(A1) to Eq.(A24) by the following substitutions

$$x_2 \leftrightarrow x_3, b_2 \leftrightarrow b_3, r_{D_{s_0}^*} \leftrightarrow r_{D_s}. \tag{B16}$$

-
- [1] B. Aubert *et al.*(BABAR Collaboration), Phys. Rev. Lett. **90**,242001 (2003).
 - [2] D. Besson *et al.*(CLEO Collaboration), Phys. Rev. D **68**, 032002 (2003).
 - [3] P. Krokovny *et al.*(Belle Collaboration), Phys. Rev. Lett. **91**, 262002 (2003).
 - [4] B. Aubert *et al.*(BABAR Collaboration), Phys. Rev. Lett. **93**, 181801 (2004).
 - [5] S.K. Choi *et al.*(BABAR Collaboration), Phys. Rev. D **91**, 092011 (2015).
 - [6] P.A. Zyla *et al.*(Particle Data Group), Prog. Theor. Exp. Phys. **2020**, 083C01 (2020).
 - [7] S. Godfrey and N. Isgur, Phys. Rev. D **32**, 189 (1985); S. Godfrey and R. Kokoski, Phys. Rev. D **43**, 1679 (1991); J. Zeng, J. W. Van Orden and W. Roberts, Phys. Rev. D **52**, 5229 (1995); D. Ebert, V.O. Galkin and R.N. Faustov, Phys. Rev. D **57**, 5663 (1998).
 - [8] Y.S. Kalashnikova, A.V. Nefediev and Y.A. Simonov, Phys. Rev. D **64**, 014037 (2001); M.Di Pierro and E.Eichten, Phys. Rev. D **64**, 114004 (2001).
 - [9] G.S. Bali, Phys. Rev. D **68**, 071501 (2003); A. Dougall *et al.* [UKQCD Collaboration], Phys. Lett. B **569**, 41 (2003).
 - [10] M. Ablikim, *et al.*[BESIII Collaboration], Phys. Rev. D **97**, 051103 (2018).
 - [11] P. Colangelo, F. De Fazio, and A. Ozpineci, Phys. Rev. D **72**, 074004 (2005).
 - [12] F. Jugeau, A. Le Yaouanc, L. Oliver, and J. C. Raynal, Phys. Rev. D **72**, 094010 (2005).

- [13] G. Herdoiza, C. Mcneile, and C. Michael (UKQCD Collaboration), *Phys. Rev. D* **74**, 014510 (2006).
- [14] P. Colangelo, G. Nardulli, A.A. Ovchinnikov, and N. Paver, *Phys. Lett. B* **269**, 201 (1991).
- [15] R.C. Hsieh, C.H. Chen, and C.Q. Geng, *Mod.Phys.Lett. A* **19**, 597 (2004).
- [16] G.S. Bali, S. Collins, A. Cox, and A. Schafer, *Phys. Rev. D* **96**, 074501 (2017).
- [17] J. Segovia, C. Albertus, E. Hernandez, F. Fernandez, and D. R. Entem, *Phys. Rev. D* **86**, 014010 (2012).
- [18] S. Veseli and I. Dunietz, *Phys. Rev. D* **54**, 6803 (1996).
- [19] R.C. Verma, *J. Phys. G* **39**, 025005 (2012).
- [20] H.Y. Cheng, C.K. Chua, and C.W. Hwang, *Phys. Rev. D* **69**, 074025 (2004).
- [21] H.Y. Cheng and W.S. Hou, *Phys. Lett. B* **566**, 193 (2003).
- [22] A. Faessler, T. Gutsche, S. Kovalenko, V.E. Lyubovitskij, *Phys. Rev. D* **76**, 014003 (2007).
- [23] A. Le Yaouanc, L. Oliver, O. Pene, J.C. Raynal, and V. Morenas, *Phys. Lett. B* **520**, 59 (2001).
- [24] T. Barnes, F. E. Close, and H.J. Lipkin, *Phys. Rev. D* **68**, 054006 (2003).
- [25] Y.Q. Chen, and X.Q. Li, *Phys. Rev. Lett.* **93**, 232001 (2004).
- [26] F.K. Guo, P.N. Shen, H.C. Chiang, R.G. Ping, and B.S. Zou, *Phys. Lett. B* **641**, 278 (2006).
- [27] A. Faessler, T. Gutsche, V.E. Lyubovitskij, and Y.L. Ma, *Phys. Rev. D* **76**, 014005 (2007).
- [28] F.K. Guo, C. Hanhart, and U.G. Meissner, *Eur.Phys.J.A* **40**, 171 (2009).
- [29] H.Y. Cheng and W.S. Hou, *Phys. Lett. B* **566**, 193 (2003).
- [30] K. Terasaki, *Phys. Rev. D* **68**, 011501(R) (2003).
- [31] V. Dmitrasinovic, *Phys. Rev. Lett.* **94**, 162002 (2005).
- [32] J.R. Zhang, *Phys. Lett. B* **789**, 432 (2019).
- [33] E.V. Beveran and G. Rupp, *Phys. Rev. Lett.* **91**, 012003 (2003).
- [34] D. Mohler, C.B. Lang, L. Leskovec, S. Prelovsek, and R.M. Woloshyn, *Phys. Rev. Lett.* **111**, 222001 (2013).
- [35] L. Liu, K. Orginos, F.K. Guo, C. Hanhart, and U.G. Meissner, *Phys. Rev. D* **87**, 014508 (2013).
- [36] E. van Beveren, G. Rupp, *Phys. Rev. Lett.* **91**, 012003 (2003).
- [37] D.S. Hwang, D.W. Kim, *Phys. Lett. B* **601**, 137 (2004).
- [38] Z.Y. Zhou, Z. Xiao, *Phys. Rev. D* **84**, 034023 (2011).
- [39] A.M. Badalian, Yu.A. Sinonov, M.A. Trusov, *Phys. Rev. D* **77**, 074017 (2008).
- [40] M.A. Nowak, M. Rho, I. Zahed, *Acta Phys. Polon. B* **35**, 2377 (2004).
- [41] E.E. Kolomeitsev, M.F.M. Lutz, *Phys. Lett. B* **582**, 39 (2004).
- [42] W. Wei, P.Z. Huang, S.L. Zhu, *Phys. Rev. D* **73**, 034004 (2006).
- [43] M. Sadzikowski, *Phys. Lett. B* **579**, 39 (2004).
- [44] S.F. Radford, W.W. Repko, M.J. Saelim, *Phys. Rev. D* **80**, 034012 (2009).
- [45] Fayyazuddin, Riazuddin, *Phys. Rev. D* **69**, 114008 (2004).
- [46] J.B. Liu, M.Z. Yang, *Chin.Phys.C* **40**(7), 073101 (2016).
- [47] A. Zhang, *Phys. Rev. D* **72**, 017902 (2005).
- [48] H.X. Chen, W. Chen, X. Liu, Y.R. Liu, S.L. Zhu, *Rept. Prog. Phys.* **80**, 076201 (2017).
- [49] M.Q. Huang, *Phys. Rev. D* **69**, 114015 (2004).
- [50] Z.Q. Zhang, H.x. Guo, N. Wang, H.T. Jia, *Phys. Rev. D* **99**, 073002 (2019).
- [51] R.H. Li, C.D. Lu, Y.M. Wang, *Phys. Rev. D* **80**, 014005 (2009).

- [52] S.M. Zhao, X. liu, S.J. Li, Eur. Phys. J. C **51**, 601 (2007).
- [53] Y.L. Shen, Z.J. Yang, X. Yu, Phys. Rev. D **90**, 114015 (2014).
- [54] C. Albertus, Phys. Rev. D **89**, 065042 (2014).
- [55] C.H. Chen, Phys. Rev. D **68**, 114008 (2003).
- [56] R.N. Faustov, V.O. Galkin, Phys. Rev. D **87**,034033 (2013).
- [57] Y.Y. Keum, H.n. Li and A.I. Sanda, Phys. Lett. B **504**, 6 (2001)
- [58] A. Ali, G. Kramer, Y. Li, C.D. Lu, Y.L. Shen, W. Wang and Y.M. Wang, Phys. Rev. D**76**, 074018 (2007).
- [59] C.D. Lu, M.Z. Yang, Eur. Phys. J. C**28**, 515 (2003).
- [60] T. Kurimoto, H.n. Li and A.I. Sanda, Phys. Rev. D **67**, 054028 (2003).
- [61] R.H. Li, C.D. Lu, H. Zou, Phys. Rev. D **78**, 014018 (2008).
- [62] H.Y. Cheng, C.K. Chua, Phys. Rev. D **74**, 034020 (2006).